Supplementary Material

Appendix – [A]: Summary of Input data for the Beam-on-Nonlinear-Winkler-Foundation (BNWF) model in ABAQUS (2020).

This Appendix summarises the input data that describe the interaction properties (spring nonlinear stiffnesses and calibrated dashpots) and the boundary condition dynamic amplitudes of the BNWF model in ABAQUS. For additional details about how these data were determined, the reader is encouraged to refer to previous work by the authors (Mubarak 2023; Mubarak et al. 2025).

1. Ground-structure interaction properties (nonlinear springs stiffnesses in all orthogonal directions), including the CMS cavern and the LHC tunnel (Figure A1):

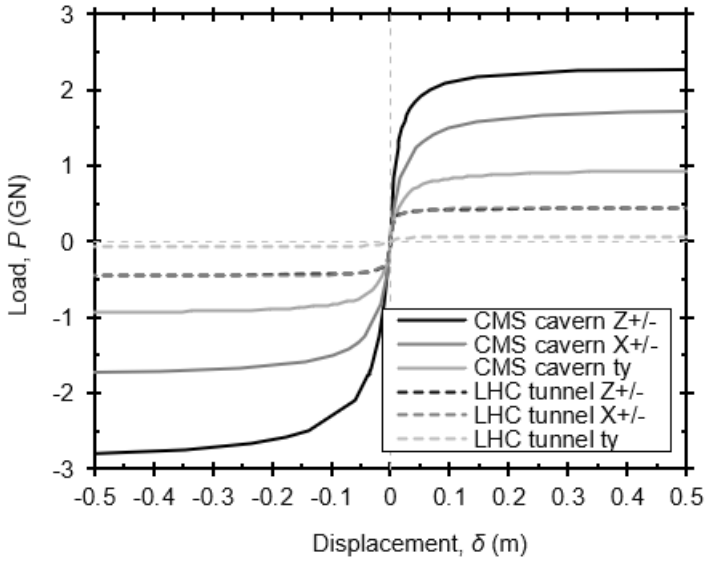

Figure A1 Nonlinear spring properties for the CMS caven and LHC tunnel structures.

2. Ground-structure interaction properties for the vertical shafts passing through Rock and Moraine layers (Figure A2):

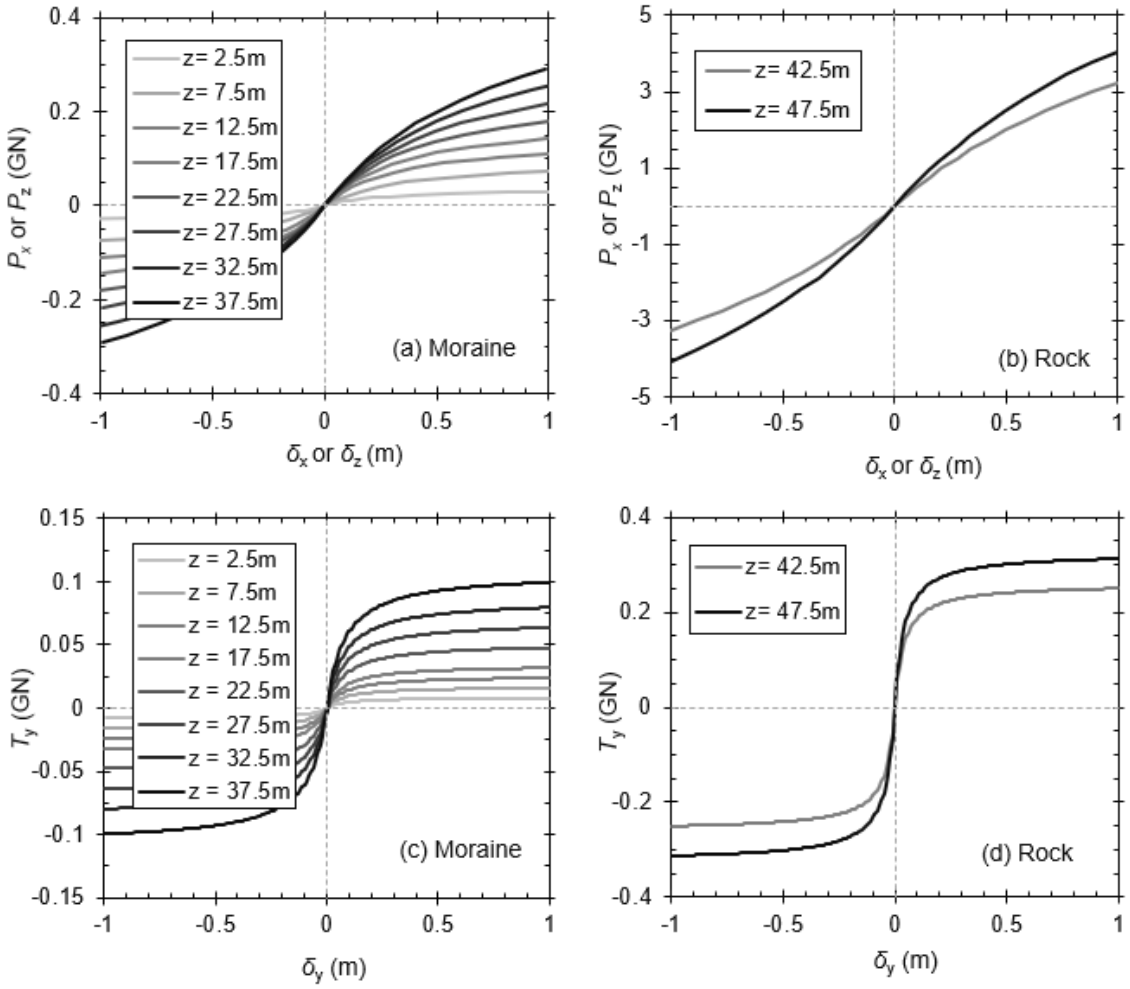

Figure A2 (a) & (b) transverse nonlinear spring stiffnesses in rock and moraine, and (c) & (d) axial nonlinear spring stiffnesses

3. Dashpot coefficients for the Shaft. CMS cavern and the LHC tunnel that were used to represent the system damping, using frequency independent numerically calibrated values (Figure A3).

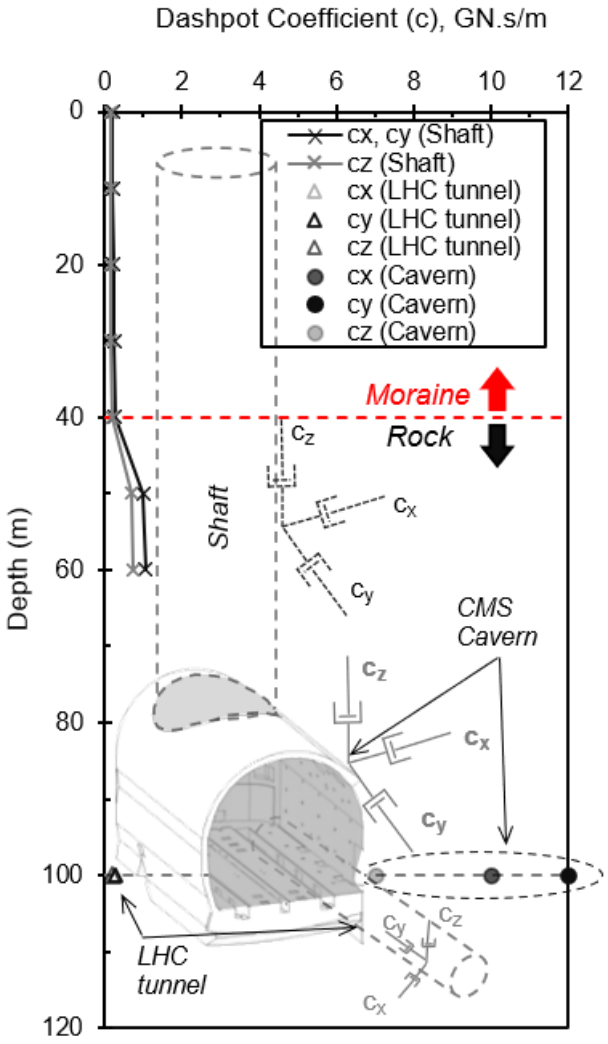

Figure A3 Numerically calibrated estimates of frequency independent dashpot constants for the shaft, CMS caven and LHC tunnel structures

4. Ground motion components of the 'Swiss motion'

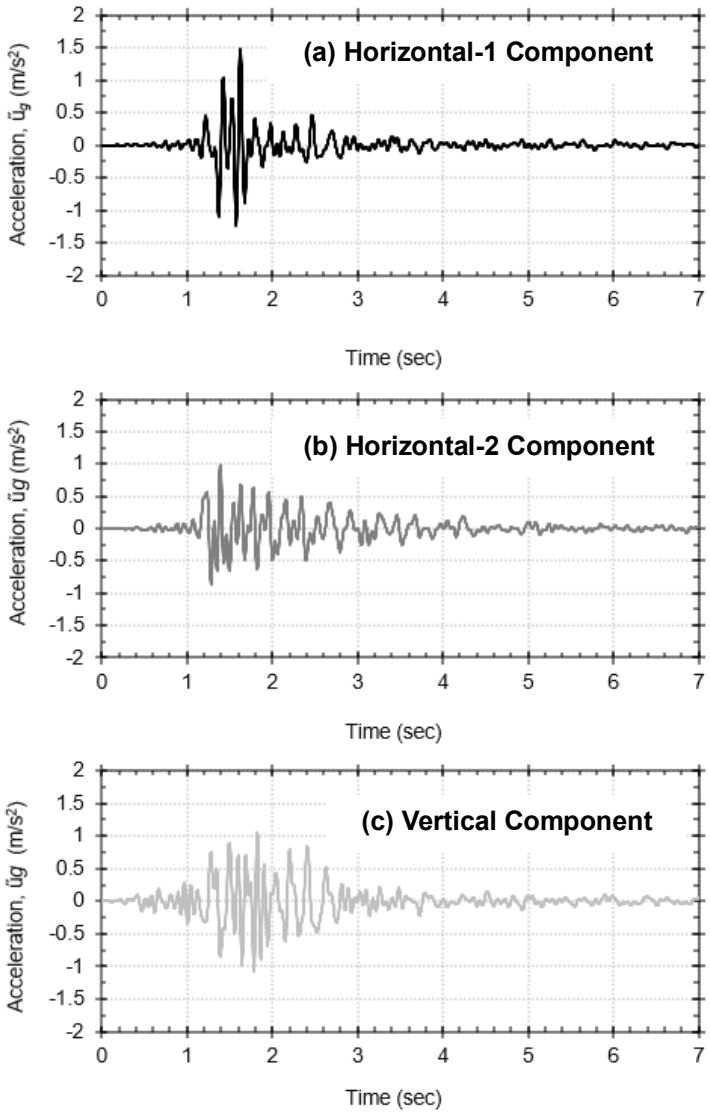

Figure A4 Local Swiss motion with the (a) dominant, (b) secondary horizontal and (c) vertical acceleration components.

5. Dynamic displacements (amplitudes) used at the free boundary points of the springs in all orthogonal directions at the tunnel's elevation (~100m BGL; Figure A4).

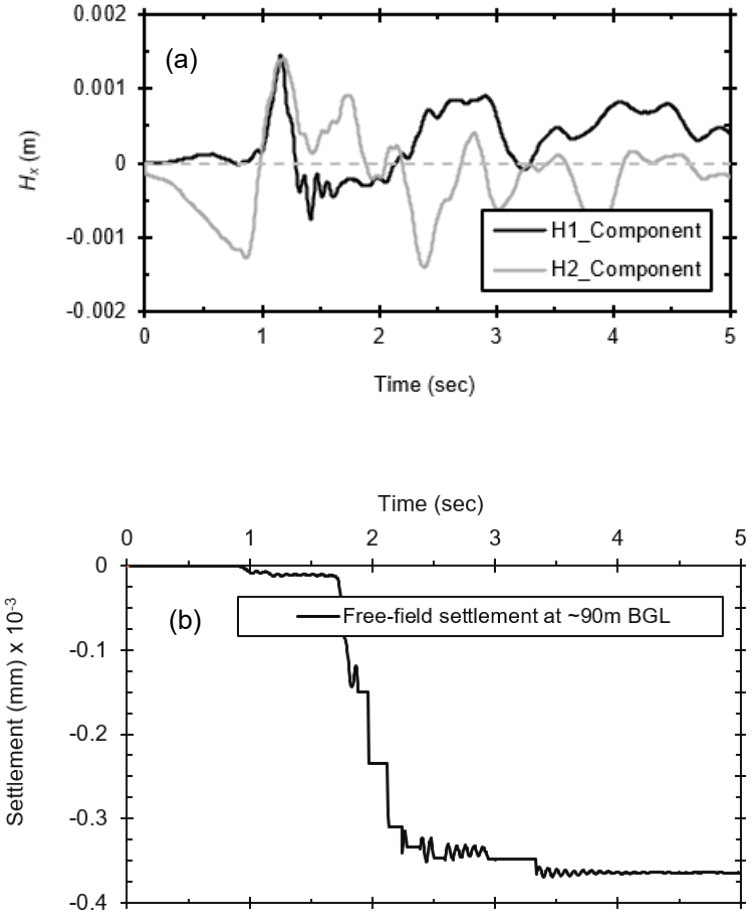

Figure A5 (a) In-plane displacement amplitude vectors (H_1(t) and H_2(t)) at the level of the tunnel (100m BGL) and (b) out-of-plane displacement vector V(t).

6. Dynamic displacements (amplitudes) used at the free boundary points of the springs in all orthogonal directions for the vertical shafts at different depths (Figure A5):

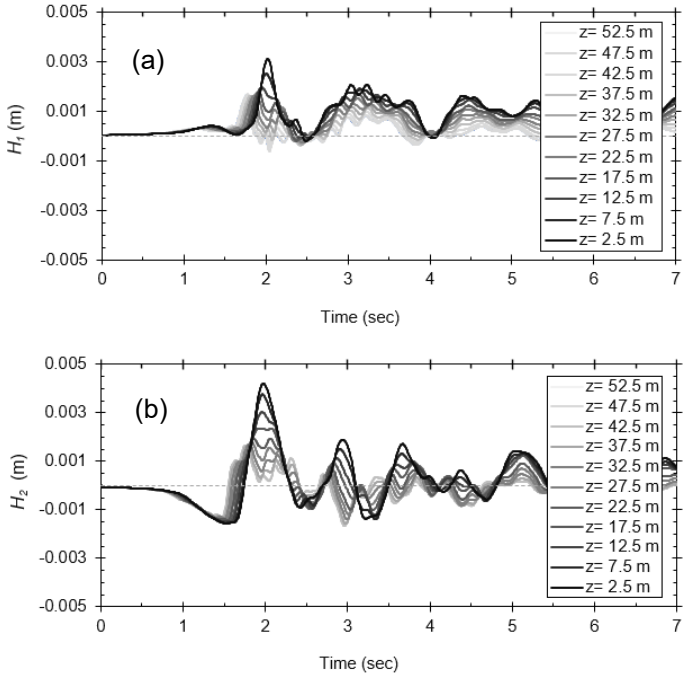

Figure A6 displacement amplitude vectors at different depths for the vertical shafts from (a) dominant 'H_1(t)' and (b) secondary 'H_2(t)' earthquake components

Table A1 Summary of the estimated shear wave velocity of the at each local station within a 60 km radius near the Geneva area (from ESM database)

Station code	Epicentral distance (km)	Arrival time (sec)	Shear wave velocity, V_s (m/s)
STSW	54.9	42	1316
SAYF	51	52	985
SALT	44.5	39	1149
SDIF	45.7	37	1234
DIX	46.2	38	1227
SMAR	18.3	17	1098
EMV	8.1	7	1240
OGSI	6.8	6	1200
OGTB	29.2	31	945
OGAN	57.4	57	1003
		Average V_a	**1140 m/s**

Appendix – [B]: Summary of Input data for the 3D FEA model boundary conditions

This Appendix summarises the Swiss motion components and the input data that were assigned to the boundaries of the 3D-FEA model of the longitudinal tunnel section which were extracted from the BNWF model of the circular LHC tunnel alignment. For additional background detail about how these data were determined, the reader is encouraged to refer to previous work by the authors (Mubarak 2023).

1. Actions at both ends of the tunnel due to Eastwards synchronous motion (Fig B1) and Asynchronous motion (Fig B2) conditions:

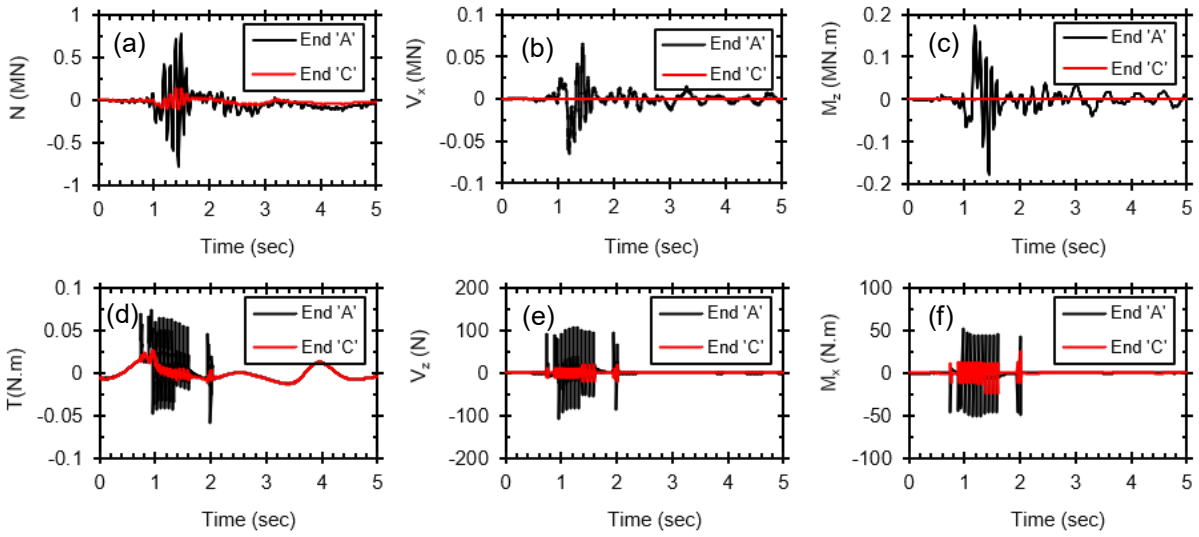

Figure B1 Time-histories of actions obtained from the BNWF model of the circular LHC alignment under synchronous motion conditions. (see **Error! Reference source not found.** in the main text)

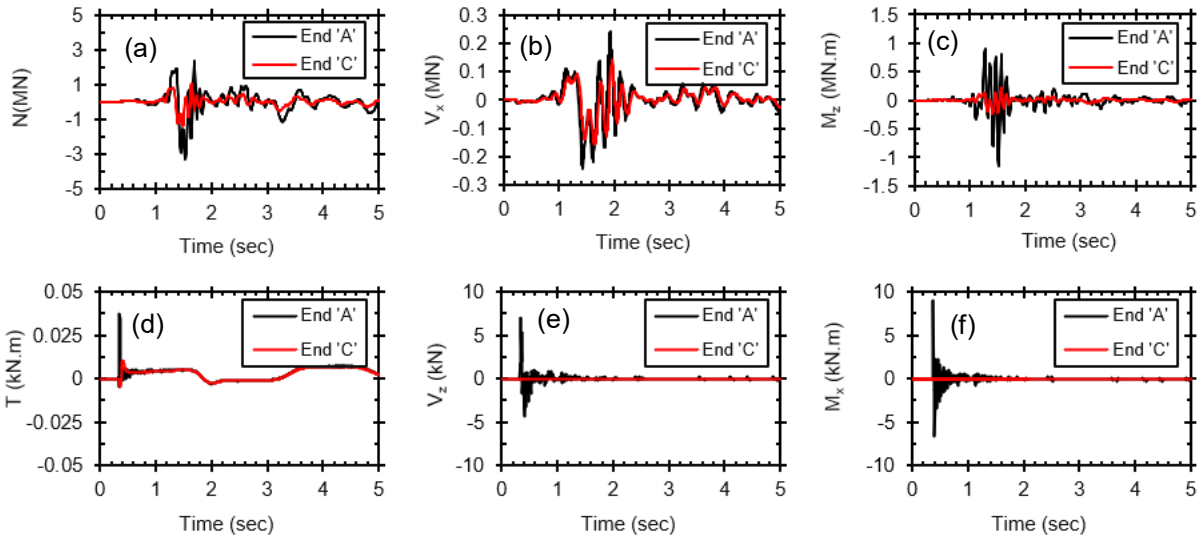

Figure B2 Time-histories of actions obtained from the BNWF model of the circular LHC alignment under asynchronous motion conditions. (see **Error! Reference source not found.** in the main text)

2. Schematic illustration for the assignment of the boundary stresses from the BNWF model to the 3D FE model boundaries (Fig B3):

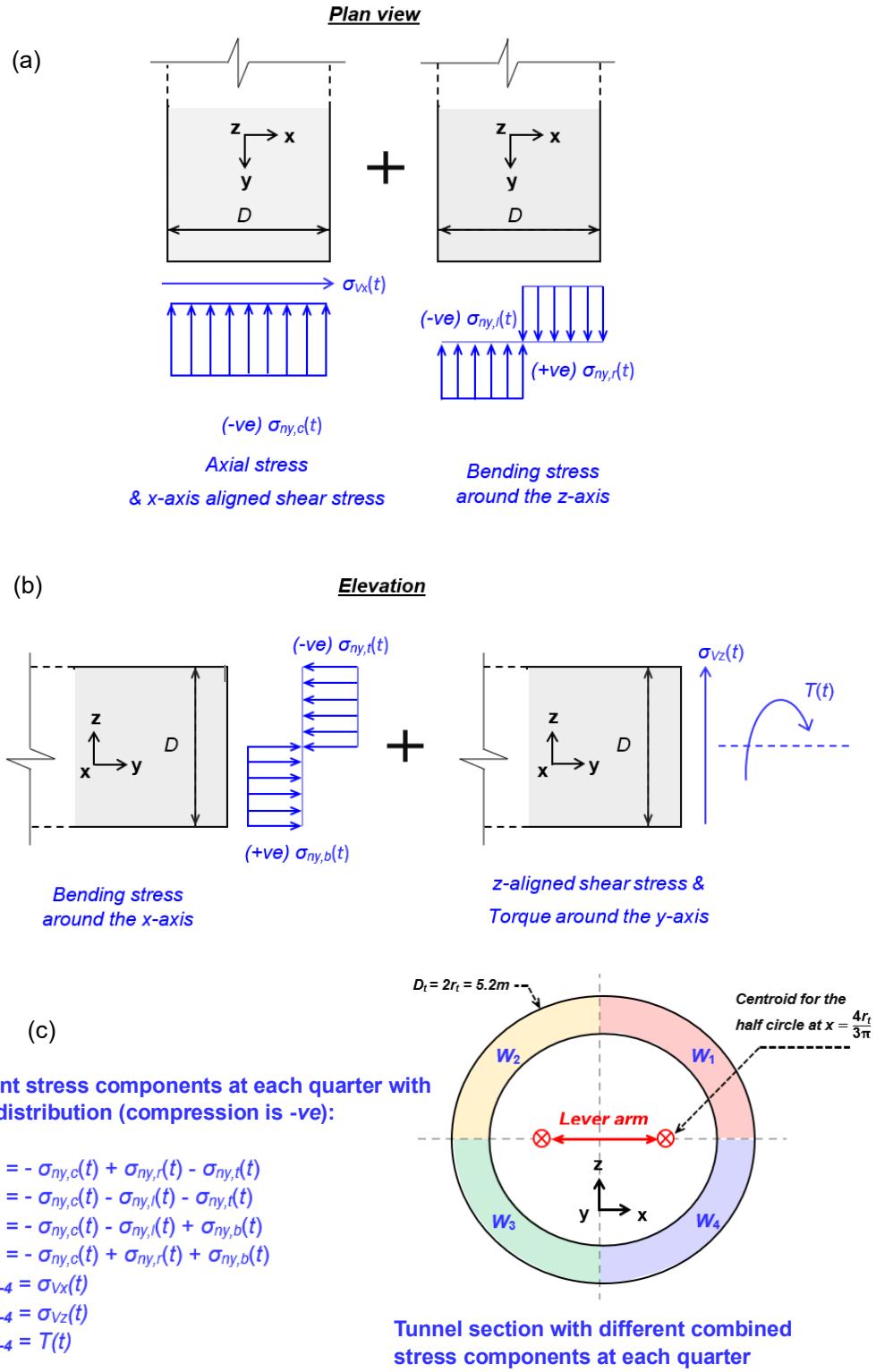

Figure B3 Schematic approach for obtaining dynamic boundary stresses from BNWF actions, where $D = 2r_t$ is the tunnel diameter (r_t = radius).

3. Equivalent boundary stresses assigned to the 3D FE longitudinal tunnel boundaries (Fig B4):

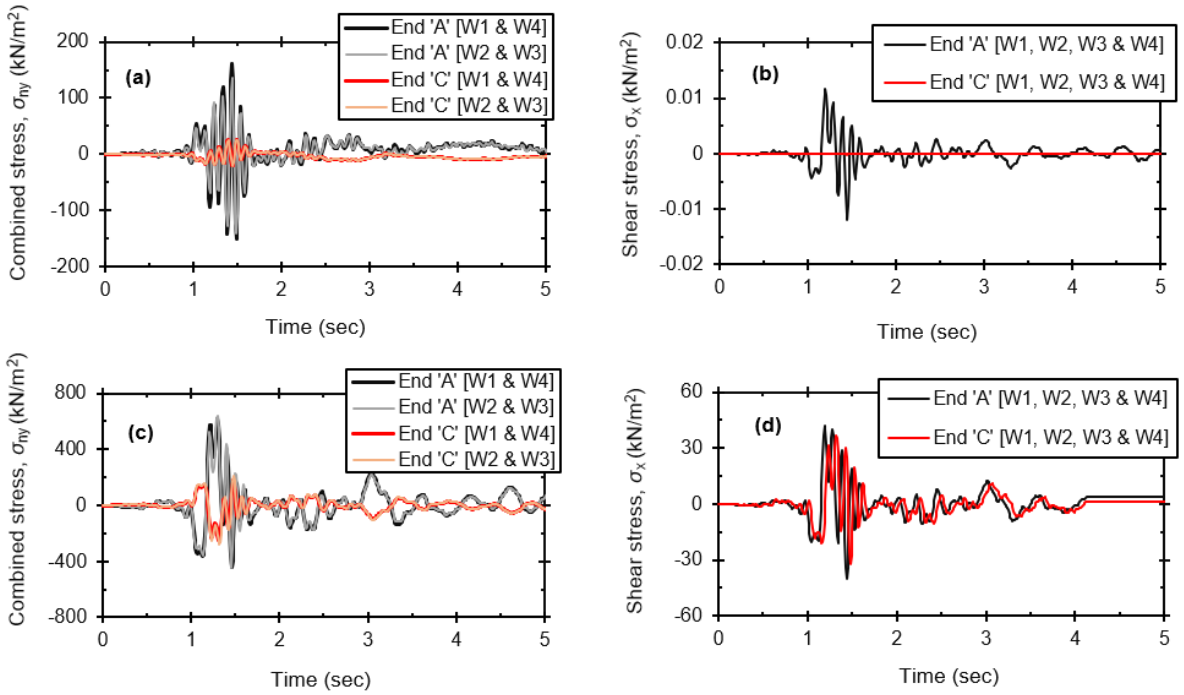

Figure B4 Equivalent boundary stress time-histories, where (a & b) are for synchronous conditions in the BNWF model, and (c & d) are for asynchronous conditions in the BNWF model.

4. Selected points at the tunnel circumference used to determine the maximum ovalisation (Fig B5):

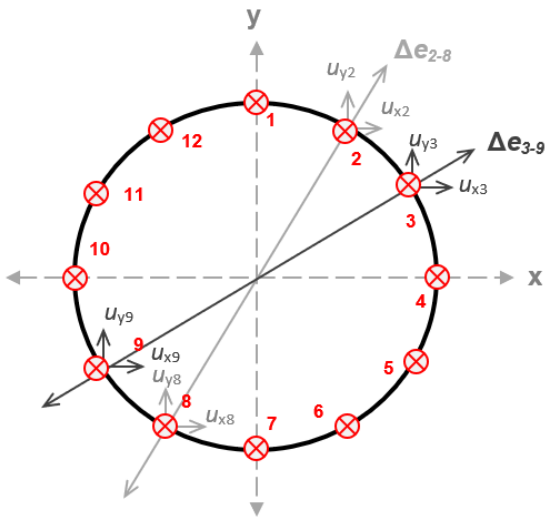

Figure B5 Selected corresponding points around the tunnel circumference to determine the time-step at which the tunnel section has the maximum ovalisation

Table B1 Summary of the Concrete Model parameters used

Description	**Parameter**	**LHC tunnel**	**Unit**
Concrete Grade	-	C25/30	MPa
28 days Young's modulus	E_{28}	25	GPa
Poisson's ratio	ν	0.2	-
Uniaxial compressive strength	$f_{c,28}$	28	MPa
Uniaxial tensile strength	$f_{t,28}$	2.8	MPa
Normalised initially mobilised strength	$\sigma_{0,c}$	0.2	-
Normalised failure strength	$\sigma_{c,c}$	0.8	-
Normalised residual strength	$\sigma_{r,c}$	0.1	-
Uniaxial plastic failure strain	ε_{cp}^{p}	-1×10^{-3}	-
Compressive fracture energy	$G_{c,28}$	50	kN/m
Tensile fracture energy	$G_{t,28}$	0.15	kN/m
Ratio of residual vs. peak tensile strength	$\sigma_{r,t}$	0	-
Maximum friction angle	ϕ_{max}	31.5	o
Dilatancy angle	ψ	11	o

Table B2 Summary of plate element properties used in the FE model

Steel property	**Top/bottom steel**	**Dummy plate**
Behaviour	Elastoplastic	Elastoplastic
EA (kN/m)	0.56×10^{6}	10.7
EI (kN.m^2/m)	17×10^{-3}	0.11
N_p (kN/m)	1224	0.18

Table B3 HS-small model parameters for different geotechnical formations at CERN's CMS site (Point-5)

Parameter	Symbol	Unit	Molasse rock	
			Med.-strong	Strong
Unconfined compressive strength of intact rock	σ_{ci}	MPa	15 ± 3.9	25 ± 5.5
Saturated Unit weight	γ_{sat}	kN/m^3	24	24
Secant stiffness (drained triaxial)	E_{50}^{ref}	kN/m^2	1.2×10^6	3.4×10^6
Tangent stiffness (oedometer)	E_{oed}^{ref}	kN/m^2	960×10^3	2.7×10^6
Unloading/reloading stiffness	E_{ur}^{ref}	kN/m^2	3.4×10^6	10.2×10^6
Reference shear modulus	G_0^{ref}	kN/m^2	2.7×10^6	4.1×10^6
Shear strain at (70% G_0)	$\gamma_{0.7}$	[-]	1.2×10^{-3}	1.2×10^{-3}
Apparent cohesion	c'_{ref}	kN/m^2	2000	3000
Friction angle	φ'	[°]	41	48
Dilatancy angle	ψ	[°]	16	16
Poisson's ratio	ν	[-]	0.3	0.4
Power for stress-level dependency of stiffness †	m	[-]	0	0

† The power m=0 provides a constant value of the stiffness with depth (mean value) in each layer based upon a shear wave velocity profile by Fern et al. 2018.

φ' represents the equivalent friction angle of Mohr-Coulomb fit to Hoek-Brown envelope of each rock unit.